Development 138, 4039-4050 (2011) doi:10.1242/dev.069187

Vreteno, a gonad-specific protein, is essential for germline development and primary piRNA biogenesis in *Drosophila*

Andrea L. Zamparini[1,*], Marie Y. Davis[1,*,†], Colin D. Malone[1,2], Eric Vieira[1,‡], Jiri Zavadil[3], Ravi Sachidanandam[4], Gregory J. Hannon[2] and Ruth Lehmann[1,§]

SUMMARY

In *Drosophila*, Piwi proteins associate with Piwi-interacting RNAs (piRNAs) and protect the germline genome by silencing mobile genetic elements. This defense system acts in germline and gonadal somatic tissue to preserve germline development. Genetic control for these silencing pathways varies greatly between tissues of the gonad. Here, we identified Vreteno (Vret), a novel gonad-specific protein essential for germline development. Vret is required for piRNA-based transposon regulation in both germline and somatic gonadal tissues. We show that Vret, which contains Tudor domains, associates physically with Piwi and Aubergine (Aub), stabilizing these proteins via a gonad-specific mechanism that is absent in other fly tissues. In the absence of *vret*, Piwi-bound piRNAs are lost without changes in piRNA precursor transcript production, supporting a role for Vret in primary piRNA biogenesis. In the germline, piRNAs can engage in an Aub- and Argonaute 3 (AGO3)-dependent amplification in the absence of Vret, suggesting that Vret function can distinguish between primary piRNAs loaded into Piwi-Aub complexes and piRNAs engaged in the amplification cycle. We propose that Vret plays an essential role in transposon regulation at an early stage of primary piRNA processing.

KEY WORDS: Germline stem cell, Soma, Transposon, Piwi, Aubergine, piRNAs, Tudor, *Drosophila*

INTRODUCTION

Propagation of all sexually reproducing organisms depends upon the faithful development and function of reproductive organs. In *Drosophila*, oogenesis requires the coordinated differentiation of two distinct cell lineages, the germline and the gonadal somatic cells, to produce an egg. The germarium, where oogenesis initiates, contains both germline and somatic stem cells. Asymmetric cell division of germline stem cells (GSCs) within the germarium generates both a stem cell and a differentiated daughter cell, the cystoblast, which gives rise to a sixteen-cell interconnected cyst (for a review, see Morrison and Spradling, 2008). One of the sixteen cells in the cyst differentiates into an egg and the remaining cells become nurse cells (King, 1970; Spradling, 1993). Somatic cell populations are intimately associated with germ cells during oogenesis: niche cells provide GSC maintenance signals and are tightly connected to GSCs via adhesion and gap junctions (Gilboa et al., 2003; Song et al., 2002; Xie and Spradling, 1998); inner sheath cells (ISCs) intermingle with the differentiating cystoblast and early dividing cysts to promote formation of the sixteen-cell cyst (Decotto and Spradling, 2005; Margolis and Spradling, 1995); follicle stem cells and their progeny, the follicle cells, surround each germline cyst as it buds off from the germarium and provide the maturing egg chamber with the positional cues needed for establishment of anterior-posterior and dorsal-ventral polarity of the embryo (Decotto and Spradling, 2005; Forbes et al., 1996; Margolis and Spradling, 1995; Roth and Schupbach, 1994; Zhang and Kalderon, 2001).

In addition to germline development, genomic integrity must be preserved to generate viable progeny. In *Drosophila*, transposable elements occupy nearly one third of the genome (Gubb et al., 1988) and mobilization of even one of almost 150 transposon classes found can lead to defects in gametogenesis and sterility (Bucheton et al., 1984; Kidwell, 1983; Pelisson, 1981; Rubin et al., 1982). Therefore, organisms have evolved small RNA-based defense systems to fight these elements (Malone and Hannon, 2009). In *Drosophila*, both germline and somatic cells of the ovary rely on Piwi proteins and their 23-29 nt Piwi-interacting RNAs (piRNAs) to combat transposon activity (Aravin et al., 2006; Girard et al., 2006; Houwing et al., 2007; Lau et al., 2006; Pelisson et al., 2007; Sarot et al., 2004; Vagin et al., 2006). All three *Drosophila* Piwi proteins, Piwi, Aubergine (Aub) and Argonaute 3 (AGO3), are expressed in germline cells, whereas Piwi is also expressed in somatic gonadal cells. Interestingly, mutations in all known piRNA pathway components lead to oocyte and embryonic patterning defects and, ultimately, to sterility, believed to be an indirect consequence of transposon-induced genomic instability and activation of a DNA double-strand break checkpoint (Klattenhoff et al., 2007; Theurkauf et al., 2006).

[1]HHMI and Kimmel Center for Biology and Medicine at the Skirball Institute, Department of Cell Biology, New York University School of Medicine, New York, NY 10016, USA. [2]Watson School of Biological Sciences and Howard Hughes Medical Institute, Cold Spring Harbor Laboratory, 1 Bungtown Road, Cold Spring Harbor, NY 11724, USA. [3]Department of Pathology, NYU Cancer Institute and NYU Center for Health Informatics and Bioinformatics, New York University Langone Medical Center, New York, NY 10016, USA. [4]Department of Genetics and Genomic Sciences, Mount Sinai School of Medicine, 1425 Madison Avenue, New York, NY 10029, USA.

*These authors contributed equally to this work
[†]Present address: Neurology Department, University of Washington Medical Center, Health Sciences Building RR650, 1959 NE Pacific Street, Seattle, Washington, WA 98195, USA
[‡]Present address: Office of Technology and Business Development, Mount Sinai School of Medicine, One Gustave L. Levy Place, New York, NY 10029, USA
[§]Author for correspondence (ruth.lehmann@med.nyu.edu)

Accepted 11 July 2011

In contrast to other small RNAs, such as microRNAs and siRNAs, which are produced from double-stranded RNA precursors, piRNAs are derived from single-stranded RNA precursors, independently of the endonuclease Dicer (Vagin et al., 2006). piRNA precursors originate from either active transposon transcripts or discrete genomic loci known as 'piRNA clusters' (Brennecke et al., 2007). In *Drosophila*, piRNA clusters provide the primary source of antisense transposon transcripts, whereas active transposons predominantly provide sense transcripts (Brennecke et al., 2007; Gunawardane et al., 2007). piRNAs associated with Piwi and Aub are mostly derived from piRNA clusters, mapping complementary to active transposons, whereas AGO3-bound piRNAs appear to be derived from the transposon itself (Brennecke et al., 2007). This relationship and a 10 nt overlap observed between sense and antisense piRNA pairs led to a model of piRNA amplification termed 'ping-pong', in which 5′ ends of new piRNAs are generated through cleavage by the Piwi proteins themselves (Brennecke et al., 2007; Gunawardane et al., 2007). In the *Drosophila* ovary, piRNA 'ping-pong' is restricted to germline cells in which Piwi, Aub and AGO3 are present, although Piwi appears to be mostly dispensable for 'ping-pong' amplification (Malone et al., 2009). In gonadal somatic cells, in which only Piwi is expressed, an alternative pathway functions. Here, single-stranded piRNA clusters or gene transcripts are processed to produce 'primary' piRNAs that are directly loaded into Piwi, targeting active transposons or endogenous genes (Li et al., 2009; Malone et al., 2009; Saito et al., 2009). The overlapping genetic requirements for Piwi in the germline and ovarian somatic cells suggest that Piwi may also engage primary piRNAs in the germline. Like Piwi, the germline-specific Aub engages piRNAs complementary to transposons, but has not been directly linked to primary piRNAs. Therefore, the precise relationship between primary piRNAs and 'ping-pong' in the germline remains largely unknown.

The restriction of piRNA production and transposon control in gonadal tissues raises the question of how the piRNA biogenesis machinery has evolved specifically in the gonad. Here, we have identified Vreteno (Vret), a gonad-specific, Tudor domain-containing protein that functions specifically in the germline and somatic gonadal tissues during oogenesis. We show that Vret broadly regulates transposon levels and has an essential role in primary piRNA biogenesis, leaving 'ping-pong' amplification intact.

MATERIALS AND METHODS

Drosophila stocks

Oregon R and w^{1118} flies served as controls. $vret^{148\text{-}60}$ and $vret^{148\text{-}15}$ were recovered from an ethyl methanesulfonate (EMS) mutagenesis screen and $vret^{15}$, $vret^{1B}$, $vret^{70}$, $vret^{39}$, $vret^{46}$ and $vret^{49}$ by non-complementation of $vret^{148\text{-}15}$. Gal4 drivers used were: *c587-Gal4* (Xie and Spradling, 1998); *nos-Gal4-VP16* (Van Doren et al., 1998); *traffic jam-Gal4* (Kyoto Stock Center); *otu-Gal4* (Rorth, 1998); and *apterous-Gal4* (from J. Treisman, NYU School of Medicine, NY, USA). *gypsy-lacZ* was a gift from A. Bucheton (CNRS, Montpellier, France); $piwi^1$ and $piwi^2$ from H. Lin (Cox et al., 1998); aub^{HN2} and aub^{QC42} (from T. Schupbach, Princeton University, NJ, USA) and *UAS-aub-gfp* from P. Macdonald (University of Texas, TX, USA). All other stocks were from the Bloomington *Drosophila* Stock Center.

Identification, mapping and molecular cloning of *vret*

vret was mapped by male mitotic recombination between P15010 and P16672, a 23 kb region uncovered by the deficiency *Df(3R)Exel 6192* (Bloomington *Drosophila* Stock Center). Single-nucleotide polymorphism (SNP) meiotic mapping between the recombinant line P15010, $vret^{1B}$ and P16672 yielded a polymorphism in the *vret* gene that identified the $vret^{1B}$ mutation.

Immunofluorescence

Adult ovaries were fixed and immunostained according to standard protocols. Wing imaginal discs immunostaining was performed as described (Roignant et al., 2006). Imaging was performed on a Zeiss Meta 510 LSM confocal microscope. All samples were stained and imaged under identical conditions.

Vret antibody production and antibody reagents

Glutathione-s-transferase-*vret* cDNA (2-367 amino acids) was isolated in inclusion bodies for production of rabbit polyclonal anti-Vret (Covance). Other antibodies used were: rabbit anti-Vasa (Lehmann laboratory) at 1:5000; mouse 1B1 monoclonal supernatant (adducin-like) (Zaccai and Lipshitz, 1996) at 1:20 and mouse anti-FasIII supernatant (7G10) at 1:10 (both from Developmental Studies Hybridoma Bank); rabbit anti-Orb (Navarro et al., 2004) at 1:500; mouse anti-Myc Alexa555 conjugated-clone4A6 (Upstate) at 1:250, mouse anti-Myc 9E10 (AbCam) at 1:1000; rabbit anti-cleaved Caspase-3 (Asp175) (Cell Signaling Technology) at 1:100; chicken anti-GFP (AVES) at 1:500; rabbit anti-GFP (Invitrogen) at 1:1000; mouse anti-β-gal (Promega) at 1:1000; rabbit anti-Piwi at 1:5000, rabbit anti-Aub at 1:1000 and rabbit anti-AGO3 at 1:1000 (all three antibodies were provided by G. Hannon) (Brennecke et al., 2007); rabbit anti-Armi (a gift from W. Theurkauf) (Cook et al., 2004) at 1:10,000; mouse anti-α-tubulin (Sigma) at 1:50,000; mouse anti-β-tubulin (Sigma) at 1:2000; mouse anti-HA (Covance) at 1:200; mouse anti-Fibrillarin (EnCor Biotechnology) at 1:500; and DAPI (Roche) at 1:500 to visualize DNA. Alexa 488-conjugated Phalloidin (Molecular Probes) was used at 1:500. Secondary antibodies coupled to Alexa 488, Cy3 or Cy5 (Jackson ImmunoResearch Laboratories) were used at 1:500.

Clonal analysis

vret germline clones were generated using the FLP/DFS (Flippase/Dominant Female Sterile) (Chou et al., 1993) or the FLP/GFP-marked clone (Xu and Rubin, 1993) systems. For FLP/DFS clones, second (L2) and third (L3) instar larvae were heat shocked at 37°C for 2 hours on two consecutive days and flp^{122}; *FRT82B,* $vret^{148\text{-}60}$*/FRT82B,* ovo^{D} adult females were fattened on yeast for 3 days for daily individual egg counts. For GFP-marked clones, L2 and L3 or 1- to 3-day-old adult flies of the genotype flp^{122}; *FRT82B* $vret^{148\text{-}60}$*/FRT82B, nlsGFP* were heat-shocked at 37°C for 2 hours on two consecutive days. Adult females were dissected 7 days after eclosion (when heat shock was carried out at larval stages) or 5 to 10 days after heat shock (when heat shock was carried out on 1- to 2-day-old adults).

Generation of transgenic flies

Full-length *vret* coding sequence from expressed sequence tag (EST) LD38352 [*Drosophila* Genomics Resource Center (DGRC)] and *5x-myc* were amplified by PCR separately and subcloned into pGEM-7Zf (Promega) for sequencing. The *vret-myc* insert was then cloned into p*UASp* (Rorth, 1998). Full-length *piwi* coding sequence from EST RE21038 (DGRC) was amplified by PCR, cloned and recombined into the pPHW vector. Both *pUASp-vret-myc* and *pUASp-HA-piwi* transgenes were introduced into the *Drosophila* genome using standard P-element-mediated transformation techniques (Rubin and Spradling, 1982). Transgene functionality was verified by complementation of sterility phenotype in the respective mutant backgrounds.

Microarray data analysis

Microarray analysis was performed in biological duplicates using total RNA extracted from *Drosophila* ovaries. The Affymetrix 3′-IVT Express Kit labeling protocol was applied followed by standardized hybridization and processing protocols using Affymetrix *Drosophila* 2.0 arrays. Transposable elements were identified on the arrays and their expression was analyzed in $vret^{148\text{-}60}$/$vret^{148\text{-}60}$, $piwi^1$/$piwi^2$ and aub^{QC42}/aub^{HN2} ovaries after probe level summarization of the array intensities using a robust

multichip average (RMA) algorithm. Each mutant was baseline-normalized to its corresponding heterozygote. Fifty-five significantly modulated probe set IDs corresponding to 52 unique transposable elements were identified in at least one of the three mutants analyzed, based on the statistical difference (*t*-test, $P<0.05$, at alpha level, no multiple testing corrections applied) between homozygotes and heterozygotes for each genotype, combined with the minimum fold-change threshold (1.33, i.e. 33% change). All normalizations, statistical analyses, visualizations of hierarchical clustering results and Venn diagrams were performed in the Agilent GeneSpring GX11.5 platform. The array data is accessible from the NCBI Gene Expression Omnibus (GEO) public repository under accession number GSE30360.

Immunoprecipitation and western blot analysis

Ovaries were homogenized in NP-40 lysis buffer (150 mM NaCl, 50 mM Tris pH 8.0, 1% NP40) and the supernatant was incubated with anti-Myc tag agarose conjugate (Millipore) for 2 hours at 4°C and then washed in NP-40 lysis buffer. Samples were run on NuPAGE 4-12% Bis-Tris gradient gels (Invitrogen). Rabbit anti-Vret was used at 1:2000, mouse anti-β-Tubulin at 1:10,000, mouse anti-α-Tubulin at 1:50,000, rabbit anti-Piwi at 1:5000, rabbit anti-Aub at 1:1000, rabbit anti-AGO3 at 1:1000, rabbit anti-Armi at 1:10,000, rabbit anti-Vasa at 1:20,000, mouse anti-Myc at 1:1000, mouse anti-Fibrillarin at 1:500 and rabbit anti-Orb at 1:1000. HRP-conjugated secondary antibodies (Jackson ImmunoResearch) were used at 1:2000. An ECL-Western Blotting Detection Kit (Amersham) was used for visualization of horseradish peroxidase (HRP).

Subcellular fractionation

Ovaries were homogenized in hypotonic lysis buffer (10 mM HEPES pH 7.9, 1.5 mM $MgCl_2$, 10 mM KCl, 0.5 mM DTT) by 10-20 strokes of a glass Dounce homogenizer. The cell suspension obtained was incubated for 15 minutes on ice (homogenate fraction), centrifuged for 10 minutes at 1000 ***g*** and the supernatant was collected (cytosolic fraction). The remaining pellet was resuspended in high salt extraction buffer (20 mM HEPES pH 7.9, 25% glycerol, 420 mM NaCl, 1.5 mM $MgCl_2$, 0.2 mM EDTA, 0.5 mM DTT), centrifuged for 5 minutes at 20,000 ***g*** and supernatant was collected (nuclear fraction).

Small RNA cloning, sequencing and analysis

Small RNAs were purified, cloned and sequenced as previously described (Brennecke et al., 2007). In brief, 18-29 nt small RNAs were size-selected on a 15% polyacrylamide vertical gel, cloned and sequenced on the Illumina Genome Analyzer II platform. Small RNA sequence reads were clipped of their 3′ linker sequence and identical sequences were collapsed. Reads were mapped, allowing for zero mismatches, against the *Drosophila melanogaster* genome release 5.0. Only reads mapping to the genome, excluding unassembled heterochromatin, were used for further analysis. Reads were normalized to the total number of 20-22 nt endogenous small interfering RNAs (endo-siRNAs) derived from all 3′UTR overlapping gene transcripts, as well as the esi-1 and esi-2 endo-siRNA clusters (Czech et al., 2008; Ghildiyal et al., 2008; Okamura et al., 2008), as previously described (Malone et al., 2009). When mapping reads to the genome, no mismatches were allowed. When mapping to transposable element consensus sequences, up to three mismatches were allowed. When calculating 'ping-pong' signal [as described in Brennecke et al. (Brennecke et al., 2008)], piRNAs were mapped allowing for three mismatches. Small RNA libraries are deposited at Gene Expression Omnibus (accession number GSE30088, data sets GSM744629 and GSM744630).

Strand-specific RT-PCR and quantitative PCR

Total RNA was isolated from ovaries using TRIzol (Invitrogen) and treated with DNAfree reagent (Ambion). Expression levels of plus or minus strand-specific piRNA transcripts from clusters regions were measured as described in Klattenhoff et al. (Klattenhoff et al., 2009). Quantitative PCR (qPCR) reactions were performed using Power SYBR Green PCR Master Mix (Applied Biosystems) with the ABI Prism 7900 system (AME Bioscience). Reactions were performed without reverse transcriptase for each sample and did not produce significant signal.

RESULTS

vreteno is required for germline and ovarian soma development

CG4771 (hereby known as *vreteno*, the Bulgarian word for 'wool-spinning spindle', referring to its eggshell phenotype) was identified in a screen for maternal-effect mutations causing defects in oocyte polarity [see Materials and methods in Staeva-Vieira (E. Staeva-Vieira, PhD thesis, New York University, 2003)]. Point mutations were identified in the *vret* coding sequence for all eight alleles (Fig. 1A; see Tables S1, S2 in the supplementary material). Both female and male *vret* mutants are sterile. Females mutant for strong *vret* alleles lay no eggs, whereas mutants for weaker alleles produce 'ventralized' eggs: the chorionic appendages, a marker for dorsal fate, were either fused or failed to form completely, a phenotype referred to as 'spindle' (see Table S1 in the supplementary material). Fertility was rescued in *vret* mutant females and males by a single copy of *vret* using a *UASp-vret-myc* transgene driven by the ubiquitously expressed *actin5C-Gal4* driver (see Table S3 in the supplementary material).

In *vret* mutant ovaries, both germline and somatic gonadal cell development is affected. In the strongest *vret* alleles ($vret^{148\text{-}60}$, $vret^{15}$, $vret^{1B}$), the germarium was filled with germ cells that maintained a round spectrosome, suggesting failure of GSCs to differentiate (Fig. 1B,D). Moreover, ISCs failed to associate with germ cells (Fig. 1D; see Fig. S2B in the supplementary material). Weaker *vret* mutants ($vret^{70}$, $vret^{39}$, $vret^{46}$) progressed to later stages of oogenesis but egg chambers were defective with abnormal nurse cell numbers and improper oocyte positioning (Fig. 1C,E,F). In these mutants, follicle cells often failed to encapsulate egg chambers (Fig. 1E), and occasionally formed disorganized multicellular layers (Fig. 1G). Finally, $vret^{49}$ *and* $vret^{148\text{-}15}$ produced ventralized eggs but showed no defects in somatic gonadal cell patterning, germ cell differentiation or oocyte specification (see Table S1 in the supplementary material).

Vret is a novel Tudor protein

Vret contains two C-terminal Tudor domains (Fig. 1A), conserved motifs composed of four β strands forming an aromatic cage known to recognize and bind symmetrically dimethylated arginine residues (sDMA) (Liu et al., 2010; Maurer-Stroh et al., 2003). Alignment of the two Tudor domains in Vret [amino acids 376 to 422 (Vret tud1) and 581 to 626 (Vret tud2)] with other Tudor domain proteins suggests that they form an N- and C-terminally 'extended' structure (referred to as eTud) that closely resembles that of Tudor-SN (hSMN) and Tudor domain 11 of *Drosophila* Tudor protein (tud11) (see Fig. S1A-B in the supplementary material) (Friberg et al., 2009; Liu et al., 2010; Shaw et al., 2007). However, both Vret Tudor domains are unusual, as they do not have all of the four aromatic residues found in the canonical Tudor domain cage (see Fig. S1A in the supplementary material). Vret tud1 has three of the four aromatic residues, and Vret tud2 has only two. Three of the four Vret missense mutations ($vret^{39}$, $vret^{49}$ and $vret^{148\text{-}15}$) map to the Tudor domains (Fig. 1A), suggesting that both domains play an important role in Vret function. Indeed, the same glycine residue is mutated in the Vret tud1 and Vret tud2 domains in $vret^{39}$ and $vret^{148\text{-}15}$, respectively, allowing a direct comparison of the relative role of the two domains. This glycine is highly conserved among Tudor domains and is likely to be important for holding the extended Tudor domain in a rigid structure (Liu et al., 2010). Interestingly, a glycine to glutamic acid change in Vret tud1 ($vret^{39}$) exhibits a stronger phenotype than the same mutation in

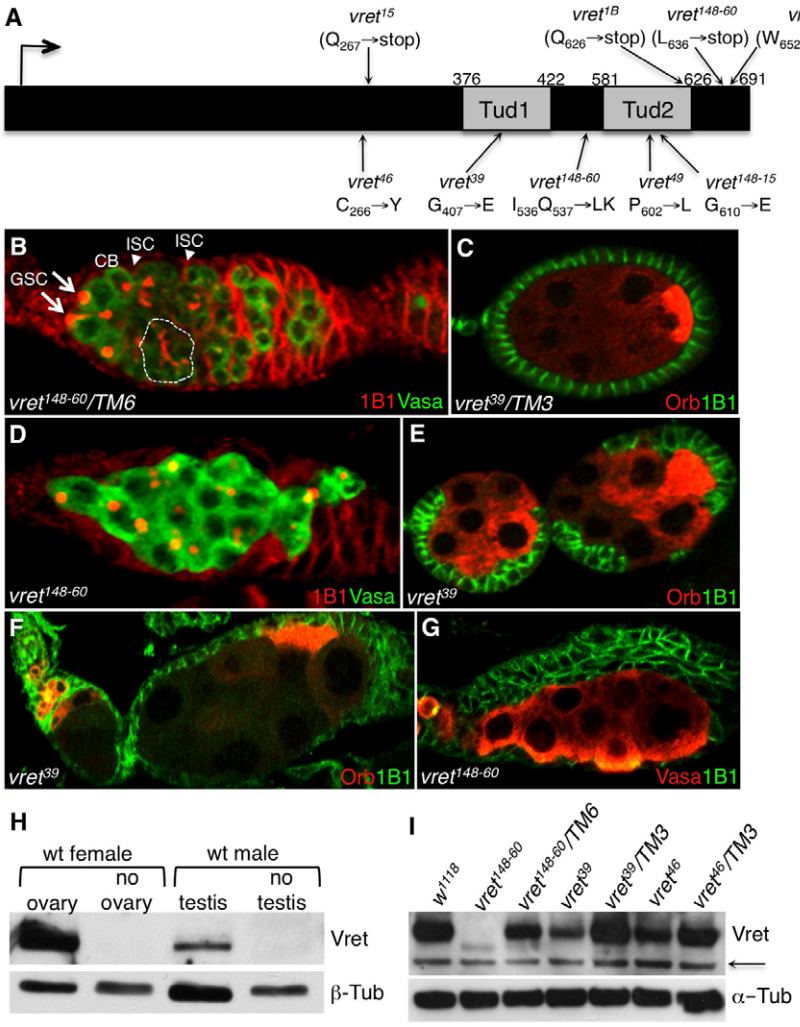

Fig. 1. *vret* is a gonad-specific, Tudor-domain protein required for germline differentiation and ovarian soma organization. (**A**) *vret* encodes a protein of 691 amino acids that includes two Tudor domains in the C terminus. *vret* stop codon mutations are indicated above and point mutations below the diagram of the protein. (**B**) In $vret^{148\text{-}60}$ heterozygotes, as in wild type, two to three GSCs with round spectrosomes are located at the anterior tip of the germarium (arrows), adjacent to the somatic niche, which is composed of terminal filaments, cap cells and ISCs (arrowheads). A cystoblast (CB) and a differentiating cyst (dashed line) are indicated. The germline is labeled with Vasa and somatic cell membranes and spectrosomes with 1B1. 1B1 staining in the GSC and CB marks single spectrosomes whereas in differentiating cysts it stains the fusome that connects the germ cells. (**C**) $vret^{39}$ heterozygote shows a normal egg chamber with an oocyte specified at the posterior, labeled by Orb, and surrounded by a somatic follicle cell epithelial layer. (**D**) Germarium filled with single, undifferentiated germ cells in $vret^{148\text{-}60}$ ovarioles. (**E**) Defective egg chambers with mislocalized oocytes and incomplete encapsulation by follicle cell layers in $vret^{39}$, a weaker *vret* allele. (**F**) $vret^{39}$ mutant exhibits an abnormal number of nurse cells and a mislocalized oocyte. (**G**) Multilayered follicle cells partially envelope nurse cells in $vret^{148\text{-}60}$ mutants. (**H**) Vret protein is detected in an immunoblot of wild-type adult ovary and testis lysates. β-Tubulin was used as loading control. (**I**) Vret antibody shows specificity in ovarian lysates of *vret* mutant alleles. Vret full-length protein (around 80 kDa) is not detectable in $vret^{148\text{-}60}$. A weak but specific band of smaller molecular weight is detected in $vret^{148\text{-}60}$, consistent with molecular data. A lower, non-specific band is observed in all samples (arrow). α-Tubulin was used as loading control.

Vret tud2 ($vret^{148\text{-}15}$). In particular, both point mutations in the Vret tud2 domain ($vret^{49}$ and $vret^{148\text{-}15}$) do not affect somatic gonadal development, suggesting a qualitatively different role of the two domains in Vret function. A fourth mis-sense mutation ($vret^{46}$) is located N-terminal to the two Tudor domains and identifies an additional region critical for Vret function.

Vret expression is gonad-specific and is required in both germline and soma for fertility

Antibodies directed against amino acids 2-367 of the Vret protein detected a discrete, 80 kDa band in extracts of wild-type ovaries and testes (Fig. 1H). Vret expression was undetectable in fly carcass, in which gonads are absent, indicating that *vret* is exclusively expressed in gonadal tissue (Fig. 1H). Full-length Vret protein was undetectable in strong mutants ($vret^{148\text{-}60}$) and reduced in weaker alleles ($vret^{39}$ and $vret^{46}$) (Fig. 1I).

To distinguish between germline and somatic roles of Vret, we generated clones of homozygous *vret* cells in an otherwise *vret*/+ background using the FLP/FRT-GFP-mediated clonal technique. Removal of Vret from the germline resulted in the eggshell patterning spindle phenotype but did not affect earlier aspects of germ cell or somatic differentiation, indicating that *vret* is required autonomously in the germline for oocyte polarity (Fig. 2A,B; see Table S2 in the supplementary material). Removal of Vret from somatic cells had no effect on oocyte specification or localization, or the morphology of the follicle cell epithelium (Fig. 2B). However, clone size and cell-lineage specificity might have prevented us from detecting a soma-specific phenotype. We therefore expressed a *UASp-vret-myc* transgene under the control of tissue-specific Gal4 drivers. As expected, no rescue of the GSC differentiation phenotype was observed when Vret was expressed under the control of germline specific drivers, such as *nos-Gal4-VP16* and *otu-Gal4* (see Table S3 in the supplementary material). By contrast, somatic drivers, including *c587-Gal4*, which drives expression in the germarial somatic cells (cap, ISCs and follicle precursor cells), and *traffic jam-Gal4*, which in addition drives expression in all follicle cells, rescued *vret* germline differentiation defects and somatic defects (see Table S3 in the supplementary material; compare Fig. 2C with 2D). Interestingly, *bab1-Gal4*, which expresses exclusively in terminal filament and cap cells, failed to rescue (see Table S3 in the supplementary material). Consistent with a role for Vret in early somatic cell lineages, we found that ISCs and accompanying somatic cells, which normally intermingle with germ cells, died in *vret* mutants as revealed by cleaved Caspase-3 expression (compare Fig. 2E with 2F). Together these results suggest that the failure in germline differentiation observed in the absence of *vret* is due to defects in the association between germ cells and their

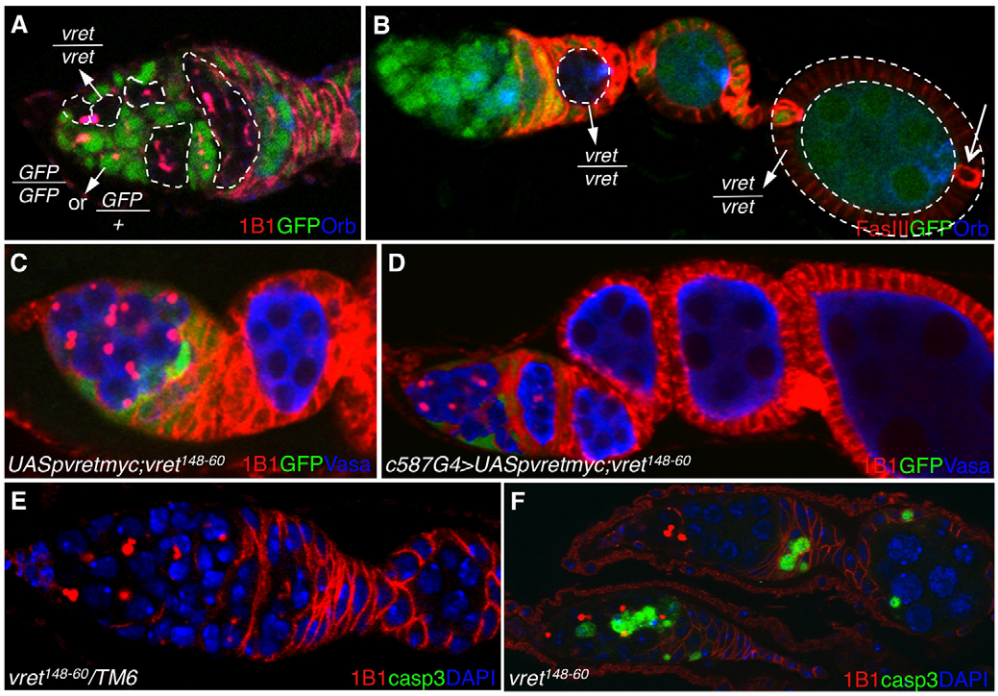

Fig. 2. *vret* is required in both soma and germline for the production of progeny. (**A**,**B**) *vret* is not required autonomously in germ cells for GSC differentiation. *vret*$^{148\text{-}60}$ mutant clones are marked by the absence of GFP. (A) A *vret* mutant GSC clone produced normally differentiating progeny (outlined), even 5-7 days after clone induction. (B) A budding *vret* germline cyst (dashed outline in germarium) shows a properly specified and localized oocyte (indicated by Orb staining). A stage 6 egg chamber with a large *vret* follicle cell clone (outlined) shows normal follicle cell morphology and polar cell specification (arrow), marked by anti-Fas III in addition to a properly specified oocyte. (**C**,**D**) Oogenesis defects are rescued in *vret*$^{148\text{-}60}$ mutants by expression of a *UASp-vret-myc* transgene using the somatic driver *c587-Gal4* (D), compared with *vret*$^{148\text{-}60}$ mutant ovaries in the absence of the driver (C). GFP expressed by a *UASp-gfp* transgene was used to mark *c587-Gal4* somatic cell populations. (**E**,**F**) Programmed cell death is detected by cleaved Caspase-3 staining in ovaries. Somatic (and possibly also germline) cells show increased Caspase-3 staining in *vret* mutant germaria (F) compared with heterozygotes (E).

somatic support cells. Thus, Vret exhibits different tissue requirements: expression of Vret in the somatic gonad is required for germ cell differentiation, somatic gonadal cell survival and morphology, whereas Vret expression in the germline is required for oocyte and embryo polarity. Only expressing *vret* ubiquitously using *actin5c-Gal4* rescued oogenesis to fertility (see Table S3 in the supplementary material).

Vret is required for transposon silencing in germline and somatic ovarian cells

Our analysis points to striking parallels between Vret and genes affecting the *Drosophila* piRNA pathway. First, Vret contains two Tudor domains, recently shown to associate with Piwi proteins (Liu et al., 2010; Nishida et al., 2009; Reuter et al., 2009; Vagin et al., 2009; Wang et al., 2009). Second, mutations in the two germline-specific *Drosophila* Piwi proteins Aub and AGO3 show oocyte polarity defects similar to those observed in *vret* germline clones (Li et al., 2009; Wilson et al., 1996). Finally, we found that mutations in both *flamenco* (*flam*), a piRNA cluster expressed exclusively in the ovarian soma, and *piwi* exhibited phenotypes similar to those observed in *vret* mutants, including defects in germ cell differentiation, somatic cell survival and follicle cell organization (Fig. 3A-F). We therefore investigated whether *vret* has a role in regulating transposable elements activity. We analyzed the expression of the retroelement *gypsy* (Prud'homme et al., 1995), which is active in the somatic gonad and is regulated by piRNAs of the *flam* cluster, using a *gypsy-lacZ* transgenic strain (Sarot et al., 2004). While little β-galactosidase activity was observed in ovarian somatic cells of an otherwise *vret* heterozygous background (Fig. 3G), *gypsy-lacZ* accumulated significantly and specifically in the somatic epithelium of *vret* mutant ovaries (Fig. 3H). *ZAM* and *Idefix*, two other transposons regulated via the somatic Piwi/piRNA pathway (Desset et al., 2003), were also de-repressed in *vret* mutant ovaries as assayed by qPCR (data not shown).

We next tested whether *vret* was involved in global transposon regulation by performing microarray analysis. We found that most transposons contained in the *Drosophila* Genome 2.0 Array (Affymetrix), including those expressed specifically in the germline or somatic tissues of the ovary, were significantly de-repressed in *vret* homozygous mutants compared with heterozygotes (Fig. 3J; see Table S4 in the supplementary material). We also compared *vret* mutant ovaries with those of *piwi* and *aub* mutants and found numerous transposons similarly regulated in the three mutants (Fig. 3I,J; see Table S4 in the supplementary material). Piwi, like Vret, acts in both germline and somatic tissues of the gonad. Thus, similar elements were de-repressed in *vret* and *piwi* mutant ovaries, including *gypsy5*, *gtwin*, *tabor* and *ZAM*, elements known to be regulated specifically in somatic cells (Fig. 3J; see Table S4 in the supplementary material). Furthermore, elements highly de-repressed in *aub* mutants were similarly de-repressed in *vret* mutants (Fig. 3J). Our results are consistent with a role for Vret in transposon regulation in both germline and somatic tissues of the *Drosophila* gonad.

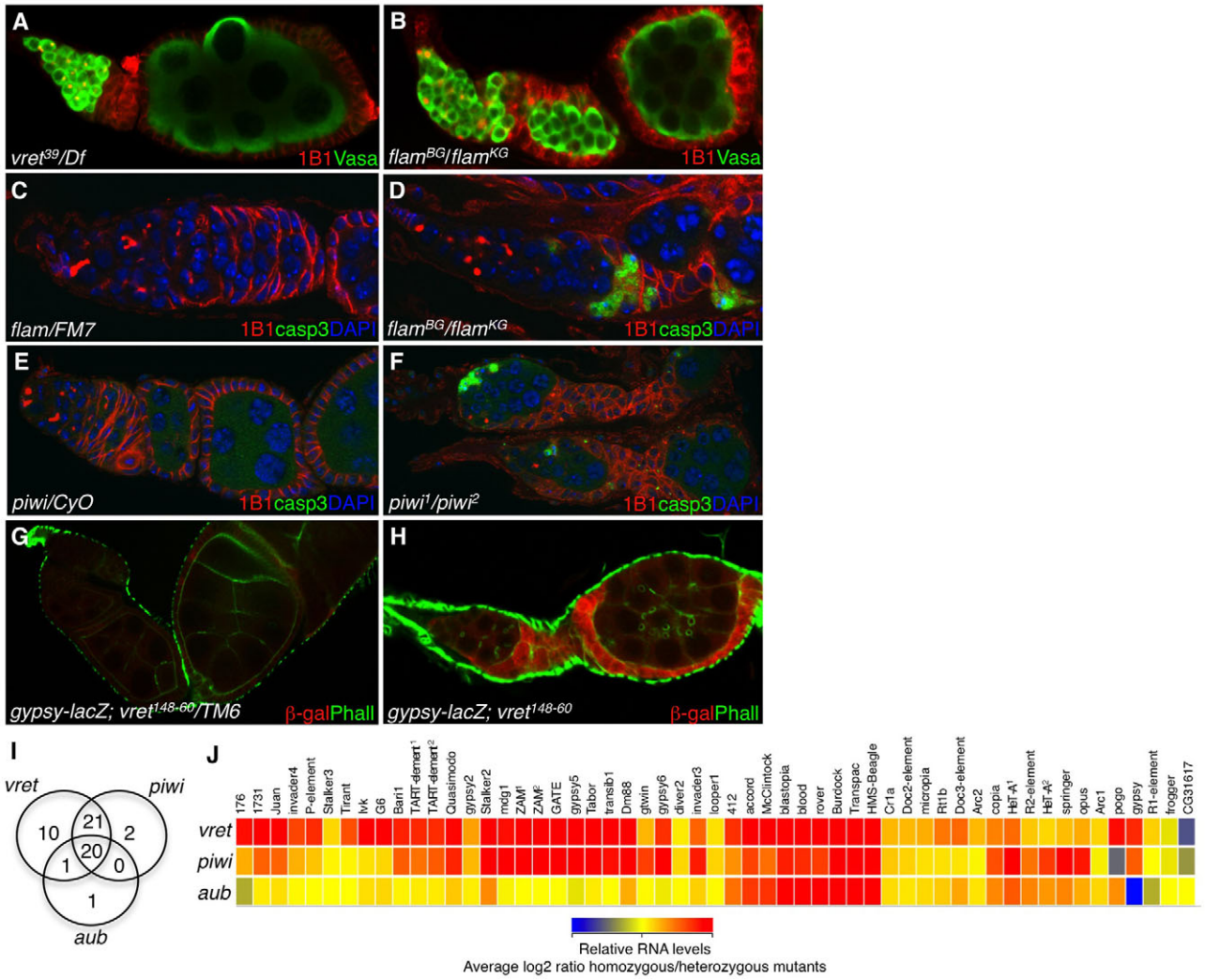

Fig. 3. *vret* is required for suppressing transposon expression in both the germline and somatic cells of the ovary. (**A**) A weak *vret* allelic combination, $vret^{39}/Df$, shows germline differentiation defects and abnormal somatic morphology. (**B**) $flam^{BG}/flam^{KG}$ mutants show defective germline and soma differentiation phenotypes, similar to *vret* mutants. (**C**,**D**) In $flam^{BG}/flam^{KG}$ mutant ovaries, somatic cells die as revealed by Caspase-3, compared with *flam* heterozygotes. (**E**,**F**) Cell death is also detected in $piwi^{1}/piwi^{2}$ mutant ovaries. (**G**,**H**) *gypsy* expression is silenced in *vret* heterozygote (G), whereas in *vret* mutants (H), *gypsy* is derepressed in somatic cells, marked by β-gal. (**I**) Venn diagram showing overlap between transposable elements regulated in *vret*, *piwi* and *aub* mutant ovaries. (**J**) Profile of transposons regulated in *vret* mutant ovaries compared with *piwi* and *aub* mutant ovaries, shown as a heat map. All homozygous or transheterozygous mutant samples were normalized to their respective heterozygotes. Note that for some transposons, more than one probe was represented on the microarray (indicated with a superscript number).

Piwi proteins localization and accumulation depend on Vret

In wild type, Aub and AGO3 are expressed exclusively in germline cells and localize to a perinuclear structure known as ‘nuage’ in nurse cells (Harris and Macdonald, 2001; Li et al., 2009; Lim and Kai, 2007). Piwi, expressed in both germline and somatic cells of the ovary, is predominantly nuclear (Brennecke et al., 2007; Cox et al., 2000). We therefore investigated whether the localization and accumulation of Piwi proteins were affected in *vret* mutants. We compared mutant and wild-type expression within the same tissue by removing *vret* specifically from germline and/or soma by clonal analysis (see Materials and methods). The nuclear localization and protein accumulation of Piwi was almost entirely abolished in *vret* germline and somatic mutant clones throughout oogenesis (Fig. 4A-B″; see Fig. S3A in the supplementary material). Aub expression was severely reduced (Fig. 4C-C″) and nuage localization was affected in mutant germline cells (see Fig. S3B in the supplementary material). By contrast, no significant change in AGO3 expression was observed (Fig. 4D-D″) although the intracellular localization of AGO3 appeared punctate (see Fig. S3C in the supplementary material).

Consistent with the clonal analysis, Piwi and Aub protein levels were reduced in western blots whereas AGO3 protein remained at wild-type levels (Fig. 4E). Protein expression of two other piRNA pathway components, Armitage (Armi) and Vasa, were unaffected by loss of *vret* (Fig. 4E). Together, these results demonstrate that *vret* is required specifically for proper localization and accumulation of Piwi and Aub protein.

Vret associates with Piwi proteins in the ovary

To determine whether Vret affects Piwi and Aub at the transcriptional level, we analyzed tagged *piwi* and *aub* transgenes under the control of the heterologous UASp promoter,

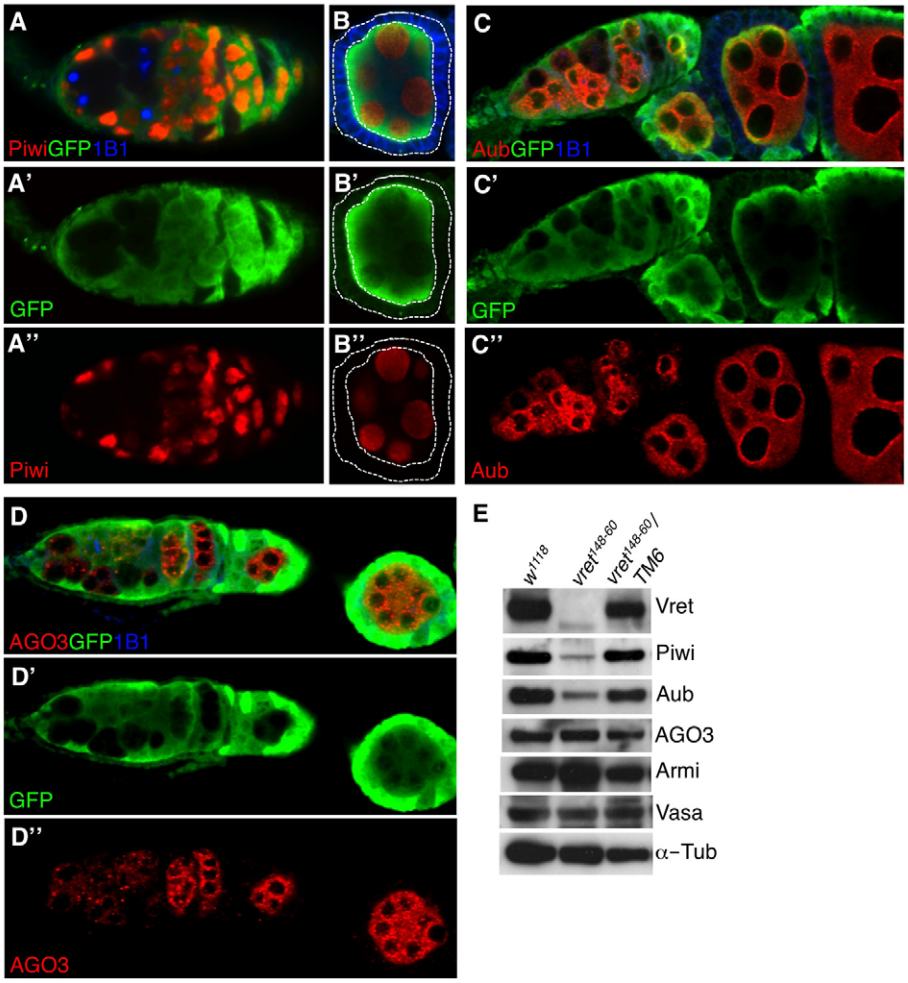

Fig. 4. *vret* is required for Piwi and Aub protein accumulation. (**A-D″**) *vret* $^{148\text{-}60}$ germline and somatic mutant clones were generated at L3 and marked by the absence of GFP. (A-B″) Germline and somatic Piwi protein expression is dramatically reduced in *vret* mutant clones. (B-B″) An egg chamber with all follicle cells mutant for *vret* shows a dramatic reduction in somatic Piwi expression (outlined). (C-C″) Aub germline expression is severely affected in *vret* germline clones, whereas AGO3 expression (D-D″) is unchanged. GFP and the proteins tested are shown in separate channels for clarity. (**E**) Protein levels of Vret, Piwi, Aub, AGO3, Armi and Vasa are shown for wild-type (w^{1118}), $vret^{148\text{-}60}$/*TM6* and $vret^{148\text{-}60}$ mutant ovaries. α-Tubulin was used as loading control.

driven by *nos-Gal4-VP16* to achieve germline expression. Transgenic Piwi and Aub proteins, revealed by Hemagglutinin (HA) and GFP staining, respectively, as well as endogenous protein levels were severely diminished in *vret* mutants (Fig. 5A-D), demonstrating that Vret is not required for *piwi* and *aub* transcription but is somehow involved in post-transcriptional stability of these proteins.

To assess whether Vret is in a complex with Piwi or Aub we immunoprecipitated Vret from ovaries and probed lysates with antibodies against piRNA pathway components. We found that Vret specifically associates with Piwi and Aub (Fig. 5E). Vret also interacts with Armi and weakly with AGO3 (Fig. 5E). Although we observed a specific interaction between Vret and the piRNA components tested, it is unclear whether they are part of the same or separate complexes.

Piwi localizes to the nucleus (Cox et al., 2000), whereas Aub is cytoplasmic and associates with the perinuclear nuage (Harris and Macdonald, 2001). Vret protein expressed from a *UASp-vret-myc* transgene appeared cytoplasmic (see Fig. S4A-D in the supplementary material). To identify the cellular compartment in which Vret, Piwi and Aub might interact, we performed subcellular fractionations. In these experiments, the cytosolic and nuclear fractions of ovarian lysates were separated by differential centrifugation (Fig. 5F). In *vret* heterozygous extracts, Vret appeared in the cytosolic fraction, marked by Orb, where it presumably associates with Aub (Fig. 5F). Piwi was found predominantly in the nuclear fraction, marked by Fibrillarin, and at lower levels in the cytoplasm (Fig. 5F), where it is most likely to interact with Vret. Piwi protein is thought to translocate to the nucleus once it is associated with piRNAs (Saito et al., 2009). By fractionating *vret* mutant ovarian extracts we found that the nuclear fraction of Piwi is affected more strongly than the cytoplasmic fraction (Fig. 5F). Since Vret is cytoplasmic, these findings suggest that Vret association with Piwi might facilitate the translocation of Piwi to the nucleus.

Piwi stabilization is regulated uniquely in the gonad

To determine whether Vret has a general role in Piwi translation or stability or it is specifically required for Piwi protein stability in the gonad, we ectopically expressed Vret and Piwi in the dorsal domain of the *Drosophila* wing disc, where neither is normally expressed (see Fig. S5A′ in the supplementary material). In this heterologous tissue, Piwi protein, expressed as a *UASp-HA-piwi* transgene, was stable in the absence of Vret (see Fig. S5C-C″ in the supplementary material). *UASp-vret-myc* transgenic expression alone was unable to induce Piwi expression, supporting the notion that *piwi* is not regulated by Vret transcriptionally or translationally (see Fig. S5B-B″ in the supplementary material). Furthermore, the expression of a *UASp-vret-myc* transgene together with *UASp-HA-piwi* did not result in an increase of Piwi levels (see Fig. S5D-D‴ in the supplementary material). These results contrast with the loss of Piwi protein in the absence of Vret in the gonad, arguing that somatic and germline cells of the gonad employ a unique surveillance pathway regulating Piwi protein stability.

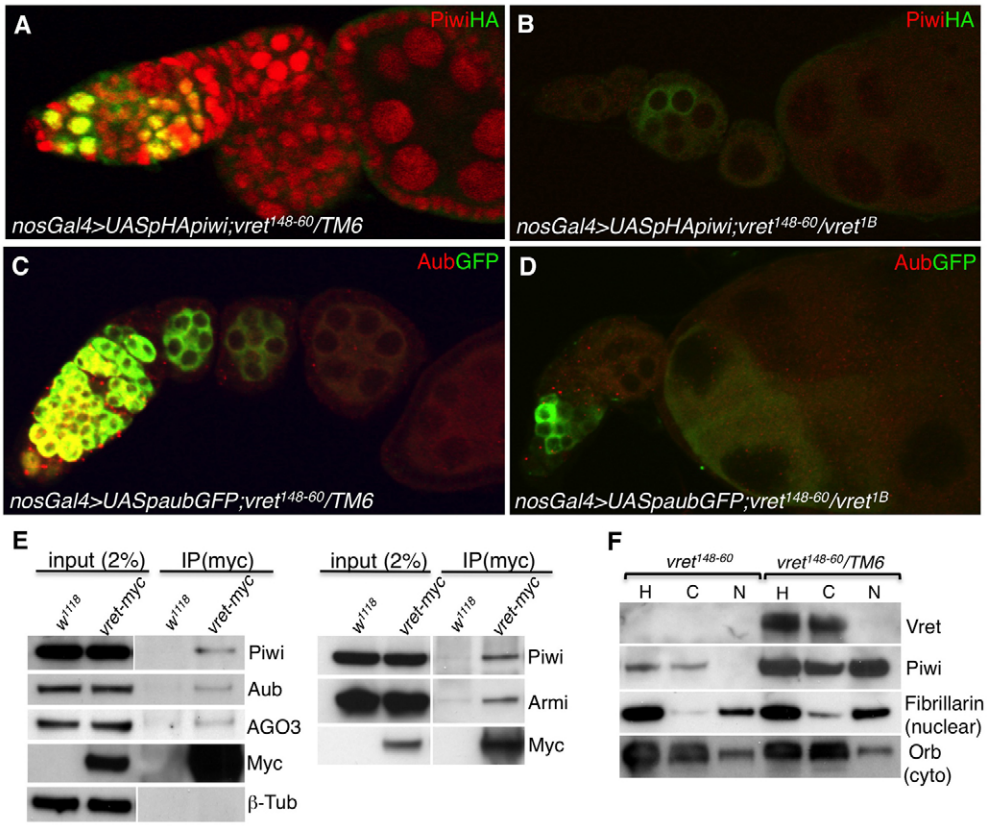

Fig. 5. Vret interacts physically with Piwi proteins and regulates their stability. (**A-D**) Post-transcriptional effects of Vret on Piwi and Aub proteins tested by expression of *piwi* and *aub* transgenes containing the UASp heterologous promoter. (A,C) Piwi and Aub proteins were expressed from *UASp-HA-piwi* and *UASp-aub-gfp* transgenes, respectively, in the germline. (B,D) Piwi and Aub protein levels are strongly reduced in *vret* mutant ovaries, shown by endogenous and transgenic expressions. (**E**) Physical interaction of Vret with piRNA components. *nos-Gal4-VP16* was used to express a *UASp-vret-myc* transgene and immunoprecipitation performed with Vret in ovarian lysates using an anti-Myc antibody. β-Tubulin was used as control. (**F**) Ovarian cell compartments can be separated by subcellular fractionation. Fibrillarin, a nuclear marker, and Orb, a cytoplasmic marker, were used as controls for efficient fraction separation. Homogenate (H), cytosolic (C) and nuclear (N) fractions are indicated. In *vret*$^{148\text{-}60}$ heterozygous ovaries, Vret appears in the cytosolic fraction whereas Piwi localizes to both nuclear and cytosolic fractions. In *vret* homozygotes, Piwi nuclear fraction is more affected than the cytosolic one.

Primary piRNA production relies on Vret

Our data show that Vret is required for Piwi and Aub stabilization, as well as transposon control, suggesting a possible role for Vret in piRNA regulation. To determine which aspect of the piRNA pathway Vret affects, we cloned and sequenced 19-29 nt small RNAs from *vret* heterozygous and homozygous ovaries, and normalized libraries to the number of gene-derived, antisense-mapping endo-siRNAs as previously described (Brennecke et al., 2007) (see Materials and methods). To account for degraded RNA contamination, when possible, we analyzed small RNAs mapping antisense to active transposons, which would probably be derived from an active processing mechanism (Malone et al., 2009). We found that small RNAs in the piRNA range (23-29 nt) were dramatically diminished (Fig. 6A). In contrast to piRNAs, we found that overall levels of siRNAs (20-22 nt) were increased. This change can, however, be almost entirely attributed to a striking increase in siRNAs derived from a single retrotransposon, MDG1 (from 0.6% to 44.2% of total siRNAs in *vret* heterozygotes compared with mutants, respectively) (Fig. 6A). The specificity of MDG1 suggests that the increase in MDG1-derived siRNAs is a product of MDG1 de-repression in the absence of piRNA silencing, rather than a more direct effect of Vret on the endo-siRNA pathway.

As piRNA clusters are the primary source of transposon-targeting piRNAs, we analyzed changes in piRNAs mapping uniquely to the genome, ensuring that they were in fact derived from the corresponding cluster (Fig. 6B,C). We found that piRNAs from germline (42AB and Cluster 3) and soma (*flam* and *traffic jam*) as well as clusters expressed in both tissues (Cluster 2) were dramatically reduced in the absence of *vret* (Fig. 6B,C).

As piRNAs bound to Piwi, Aub and AGO3 are of different average sizes (Brennecke et al., 2007) (Fig. 6D), changes in piRNA sizes can be used to determine whether Piwi-, Aub- or AGO3-bound piRNAs are differentially affected in *vret* mutants. To illustrate this point, in *aub* or *piwi* mutant ovaries, piRNAs increase or decrease in size, respectively, compared with heterozygous controls for two prototypic germline-regulated transposons, *Batumi* and *Roo* (Fig. 6E). In *vret* mutants, we observed a decrease in piRNA size compared with heterozygotes (Fig. 6E), indicating a preferential loss of Piwi-bound piRNAs and a shift towards Aub and AGO3.

Aub and AGO3 have been implicated in 'ping-pong', an amplification cycle that generates piRNAs with a 5′ complementarity between antisense and sense piRNAs. We therefore investigated whether loss of Vret affected the ability of Aub and AGO3 per se to participate in 'ping-pong'. To do this,

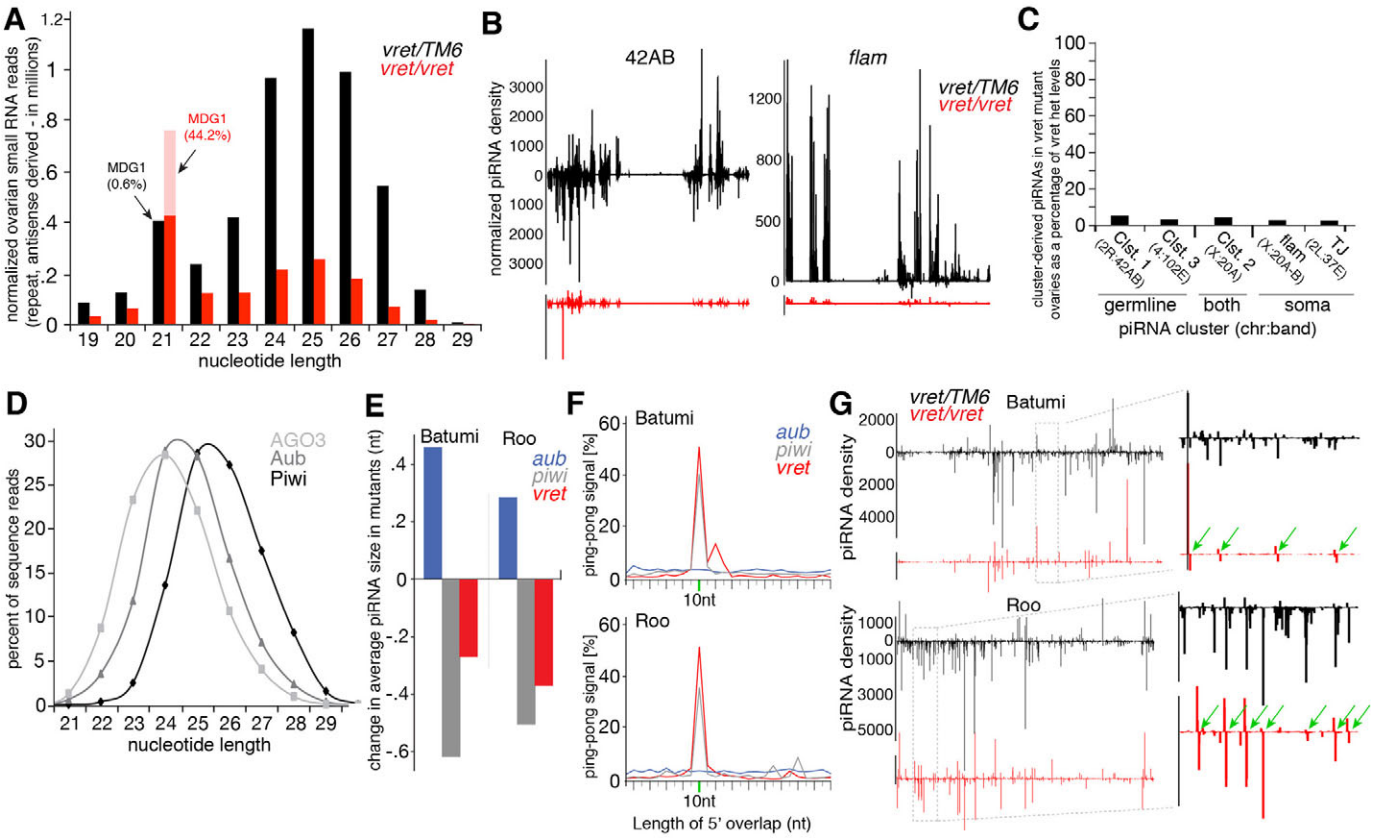

Fig. 6. Vret is required for primary piRNA biogenesis. (**A**) piRNA production is reduced in *vret* mutant ovaries. Size profiles of 'repeat, antisense mapping' annotated small RNAs from *vret*$^{148\text{-}60}$ heterozygous and *vret*$^{148\text{-}60}$ homozygous ovaries are shown. Note that increase in siRNAs derives from the transposon *mdg1* (light red) (for explanation, see text). (**B**,**C**) piRNAs generated from both germline and somatic-expressed clusters are severely reduced in *vret* mutant ovaries. (B) Density map showing normalized peaks of genome-unique piRNAs from *vret* heterozygote and mutant ovarian small RNA libraries across the 42AB (also called Cluster 1) and *flam* piRNA clusters. (C) Cluster-derived, normalized, genome-unique piRNAs remaining in *vret* mutant ovarian libraries, shown as a percentage of normalized *vret* heterozygote levels. Clusters are indicated by their cytological band location, their name, and predominant expression in either 'germline', 'soma' or 'both' types of ovarian tissues. (**D**) Size distribution of piRNAs bound by Piwi proteins. (**E**) Piwi-bound piRNAs are preferentially lost in *vret* mutant ovaries. The change in average size of ovarian, transposon-derived piRNAs, due to mutation in either *aub* (*aub*^{HN2}/*aub*^{QC42}), *piwi* (*piwi*^{1}/*piwi*^{2}) or *vret* (*vret*$^{148\text{-}60}$) is shown. Individual *aub*, *piwi* or *vret* heterozygote libraries were used to determine wild-type average piRNA size. (**F**) piRNA 'ping-pong' signal, indicated by a peak at 10 nt, from 23-29 nt reads mapping to the *Batumi* and *Roo* transposons in *aub*, *piwi* or *vret* mutant ovarian small RNA libraries. (**G**) Density map showing normalized peaks of piRNAs from *vret* heterozygote or mutant ovarian small RNA libraries, with sense mappers above the *x*-axis and antisense below. Close-ups show the remaining piRNA 'ping-pong' peaks (green arrows) in *vret* mutant ovaries compared with heterozygotes.

we measured the 5′ complementarity of piRNAs matching individual transposons, with an expected 10 nt overlap due to slicer cleavage, as previously reported (Brennecke et al., 2008). Focusing on the *Batumi* and *Roo* transposons, we observed that primary piRNAs were preferentially lost in *vret* mutants, almost exclusively leaving 10 nt offset 'ping-pong' pairs in *vret* mutant ovaries (Fig. 6F,G); this is similar to observations in *armi* and *piwi* mutants, and in contrast to *aub* mutants, which affect 'ping-pong' amplification (Fig. 6F) (Malone et al., 2009; Olivieri et al., 2010). Together, these results indicate that Vret plays an essential role upstream of Piwi, and possibly Aub, in the primary piRNA pathway. Additionally, piRNA loss is most likely to underlie the transposon silencing defects observed in *vret* mutants.

Vret does not affect piRNA cluster transcription

To determine whether piRNA cluster transcription was affected in *vret* mutants, we analyzed the steady-state RNA levels of *Drosophila* piRNA clusters by qPCR. We focused on the uni-strand-transcribed, somatic *flam* cluster and the dual-strand-transcribed, germline 42AB cluster (see Fig. S6 in the supplementary material). Ovaries mutant for *rhino* (*rhi*), which is required for cluster 42AB transcription (Klattenhoff et al., 2009), and for *flam*, in which *flam* transcript is undetected (Brennecke et al., 2007), were used as controls (see Fig. S6C,D in the supplementary material). In contrast to these controls, *vret* mutants showed no change in transcription from both the 42AB and *flam* clusters compared with heterozygotes (see Fig. S6A,B in the supplementary material), suggesting that Vret does not affect piRNA cluster transcription.

DISCUSSION

We identified a novel protein with critical roles in oocyte polarity, germline and soma differentiation, survival and transposon control. Vret, a Tudor-domain containing protein, associates with Piwi proteins in the cytoplasm of *Drosophila* ovarian cells and regulates their stability, as well as Piwi nuclear localization and localization of Aub to nuage. In the absence of Vret, piRNAs are dramatically reduced and transposons mobilized. By ordering the function of

Vret within the network of the piRNA-transposon-based system, we conclude that Vret functions in primary piRNA biogenesis at the stage of primary piRNA loading onto Piwi and Aub complexes.

Loss of Vret in the soma or germline has strikingly different morphological consequences. Our molecular analysis, however, suggests the same underlying cause for these defects: a failure to produce biologically active piRNAs. Morphologically, the *vret* germline phenotype resembles that of mutants defective in germline piRNA biogenesis, such as *aub*, *spnE* and *krimper* (Gillespie and Berg, 1995; Lim and Kai, 2007; Wilson et al., 1996). In these mutants, transposon mobilization activates a DNA damage checkpoint that leads to defects in transport and translation of maternal RNAs necessary for oocyte polarity and embryonic patterning (Chen et al., 2007; Ghabrial and Schupbach, 1999; Klattenhoff et al., 2007; Lim and Kai, 2007; Navarro et al., 2009). Interestingly, lack of *vret* in the soma resembles the *piwi* mutant phenotype, in which GSCs fail to differentiate as a consequence of somatic cell death, an event presumably associated with transposon misregulation. Thus, loss of *vret* in the germline and gonadal soma resembles loss of both Piwi and Aub. This, together with our findings that Vret associates with Piwi and Aub in ovarian extracts and affects the stability of both, strongly suggests that Vret regulates both proteins in a similar fashion.

Surprisingly, Vret is not required for piRNA 'ping-pong' amplification per se, suggesting that Vret might selectively interact with Aub and Piwi bound to primary piRNAs and not to those engaged in 'ping-pong'. In this scenario, it would be possible for maternally deposited Aub to initiate the 'ping-pong' cycle with AGO3, even in the absence of Vret (Brennecke et al., 2008). As some Aub protein remains in *vret* mutant ovaries, an active pool of Vret-independent Aub could maintain 'ping-pong' activity throughout the adult ovary. Therefore, we propose that a 'ping-pong'-independent pool of Aub within the cytoplasm depends upon primary piRNA loading, downstream of Vret function. It would be interesting to examine whether piRNAs associated with the Vret-dependent complex can, at any level, contribute to 'ping-pong', or whether Aub-bound primary piRNAs are functionally or enzymatically distinct from those involved in the piRNA amplification cycle.

In contrast to Aub, only a small subset of Piwi-bound piRNAs showed a 10 nt overlap with those bound to AGO3. Indeed, Piwi is genetically dispensible for 'ping-pong' and might be only marginally involved in 'ping-pong', if at all (Brennecke et al., 2007; Li et al., 2009). As Piwi slicer activity does not appear to be required for Piwi function (Saito et al., 2009), it seems most plausible that Piwi would act as a recipient, and not as an 'active' component of 'ping-pong' amplification. Regardless, the majority of Piwi-bound primary piRNAs act independently of 'ping-pong' and depend upon Vret for stability.

Our ectopic expression experiment suggests that Piwi is not 'intrinsically unstable', but becomes unstable in the gonad in the absence of Vret. Furthermore, Vret is not required for Piwi or Aub transcription or translation. Vret, therefore, could either coordinate the process of biogenesis and loading of primary piRNAs into Piwi and Aub complexes or be involved in stabilizing the mature RISC (RNA-induced silencing complex). Armi, a putative helicase, and Zucchini (Zuc), a member of the phospholipase D (PLD) family of phosphodiesterases, act like Vret in the soma and germline; they specifically affect Piwi protein stability and primary piRNA levels leaving the 'ping-pong' cycle intact (Haase et al., 2010; Malone et al., 2009; Olivieri et al., 2010; Pane et al., 2007; Saito et al., 2010). Unlike Vret, the levels of unprocessed precursor RNA from *flam* are increased in *zuc* mutants implicating Zuc in piRNA cluster transcript processing. We therefore favor the hypothesis that Vret, possibly together with Armi, is an essential component of Piwi and Aub RISC complexes. Vret is one of many Tudor domain proteins in *Drosophila* that affects piRNA biogenesis and contains conserved residues that are known to be required for binding of sDMAs found in Piwi proteins (Siomi et al., 2010). When mutated, each of these genes displays a rather distinct phenotype. Krimper and SpnE regulate transposon levels in the germline whereas fs(1)Yb is soma-specific. Vret is, at this point, the only Tudor domain protein known to be required in both tissues, suggesting a conserved and global role for this gene in piRNA regulation. It remains to be determined whether the mammalian Tudor homolog could fulfill a similar function.

Acknowledgements

We are grateful to Inés Carrera, Demián Cazalla, Ryan Cinalli, Lilach Gilboa, Thomas Hurd, Caryn Navarro, Prashanth Rangan and members of the Lehmann laboratory for helpful suggestions and discussions. We thank Frankie Kimm for assistance in cloning *vreteno* and Helene Zinszner for making the Vreteno antibody. We thank Rui-Ming Xu for support with the structural interpretation of the *vret* mutant alleles, Alexander Stark for bioinformatic support and Julius Brennecke for communicating unpublished results. We also thank NYU Genome Technology Center (supported in part by NIH/NCI P30 CA016087-30 grant) for assistance with microarrays and CSHL sequencing resources. We thank the Developmental Studies Hybridoma Bank for antibodies, the Bloomington stock collection for flies, and the *Drosophila* Genomics Resource Center for cDNA clones. R.L. and G.J.H. are HHMI investigators. G.J.H. is funded in part by grants from the NIH and a kind gift from Kathryn W. Davis.

Competing interests statement

The authors declare no competing financial interests.

Supplementary material

Supplementary material for this article is available at
http://dev.biologists.org/lookup/suppl/doi:10.1242/dev.069187/-/DC1

References

Aravin, A., Gaidatzis, D., Pfeffer, S., Lagos-Quintana, M., Landgraf, P., Iovino, N., Morris, P., Brownstein, M. J., Kuramochi-Miyagawa, S., Nakano, T. et al. (2006). A novel class of small RNAs bind to MILI protein in mouse testes. *Nature* **442**, 203-207.

Brennecke, J., Aravin, A., Stark, A., Dus, M., Kellis, M., Sachidanandam, R. and Hannon, G. J. (2007). Discrete small RNA-generating loci as master regulators of transposon activity in *Drosophila*. *Cell* **128**, 1089-1103.

Brennecke, J., Malone, C. D., Aravin, A. A., Sachidanandam, R., Stark, A. and Hannon, G. J. (2008). An epigenetic role for maternally inherited piRNAs in transposon silencing. *Science* **322**, 1387-1392.

Bucheton, A., Paro, R., Sang, H. M., Pelisson, A. and Finnegan, D. J. (1984). The molecular basis of I-R hybrid dysgenesis in *Drosophila melanogaster*: identification, cloning, and properties of the I factor. *Cell* **38**, 153-163.

Chen, Y., Pane, A. and Schupbach, T. (2007). Cutoff and aubergine mutations result in retrotransposon upregulation and checkpoint activation in *Drosophila*. *Curr. Biol.* **17**, 637-642.

Chou, T. B., Noll, E. and Perrimon, N. (1993). Autosomal P[ovoD1] dominant female-sterile insertions in *Drosophila* and their use in generating germ-line chimeras. *Development* **119**, 1359-1369.

Cook, H. A., Koppetsch, B. S., Wu, J. and Theurkauf, W. E. (2004). The *Drosophila* SDE3 homolog armitage is required for oskar mRNA silencing and embryonic axis specification. *Cell* **116**, 817-829.

Cox, D. N., Chao, A., Baker, J., Chang, L., Qiao, D. and Lin, H. (1998). A novel class of evolutionarily conserved genes defined by piwi are essential for stem cell self-renewal. *Genes Dev.* **12**, 3715-3727.

Cox, D. N., Chao, A. and Lin, H. (2000). piwi encodes a nucleoplasmic factor whose activity modulates the number and division rate of germline stem cells. *Development* **127**, 503-514.

Czech, B., Malone, C. D., Zhou, R., Stark, A., Schlingeheyde, C., Dus, M., Perrimon, N., Kellis, M., Wohlschlegel, J. A., Sachidanandam, R. et al. (2008). An endogenous small interfering RNA pathway in *Drosophila*. *Nature* **453**, 798-802.

Decotto, E. and Spradling, A. C. (2005). The *Drosophila* ovarian and testis stem cell niches: similar somatic stem cells and signals. *Dev. Cell* **9**, 501-510.

Desset, S., Meignin, C., Dastugue, B. and Vaury, C. (2003). COM, a heterochromatic locus governing the control of independent endogenous retroviruses from *Drosophila melanogaster*. *Genetics* **164**, 501-509.
Forbes, A. J., Lin, H., Ingham, P. W. and Spradling, A. C. (1996). hedgehog is required for the proliferation and specification of ovarian somatic cells prior to egg chamber formation in *Drosophila*. *Development* **122**, 1125-1135.
Friberg, A., Corsini, L., Mourao, A. and Sattler, M. (2009). Structure and ligand binding of the extended Tudor domain of *D. melanogaster* Tudor-SN. *J. Mol. Biol.* **387**, 921-934.
Ghabrial, A. and Schupbach, T. (1999). Activation of a meiotic checkpoint regulates translation of Gurken during *Drosophila* oogenesis. *Nat. Cell Biol.* **1**, 354-357.
Ghildiyal, M., Seitz, H., Horwich, M. D., Li, C., Du, T., Lee, S., Xu, J., Kittler, E. L., Zapp, M. L., Weng, Z. et al. (2008). Endogenous siRNAs derived from transposons and mRNAs in *Drosophila* somatic cells. *Science* **320**, 1077-1081.
Gilboa, L., Forbes, A., Tazuke, S. I., Fuller, M. T. and Lehmann, R. (2003). Germ line stem cell differentiation in *Drosophila* requires gap junctions and proceeds via an intermediate state. *Development* **130**, 6625-6634.
Gillespie, D. E. and Berg, C. A. (1995). Homeless is required for RNA localization in *Drosophila* oogenesis and encodes a new member of the DE-H family of RNA-dependent ATPases. *Genes Dev.* **9**, 2495-2508.
Girard, A., Sachidanandam, R., Hannon, G. J. and Carmell, M. A. (2006). A germline-specific class of small RNAs binds mammalian Piwi proteins. *Nature* **442**, 199-202.
Gubb, D., McGill, S. and Ashburner, M. (1988). A selective screen to recover chromosomal deletions and duplications in *Drosophila melanogaster*. *Genetics* **119**, 377-390.
Gunawardane, L. S., Saito, K., Nishida, K. M., Miyoshi, K., Kawamura, Y., Nagami, T., Siomi, H. and Siomi, M. C. (2007). A slicer-mediated mechanism for repeat-associated siRNA 5′ end formation in *Drosophila*. *Science* **315**, 1587-1590.
Haase, A. D., Fenoglio, S., Muerdter, F., Guzzardo, P. M., Czech, B., Pappin, D. J., Chen, C., Gordon, A. and Hannon, G. J. (2010). Probing the initiation and effector phases of the somatic piRNA pathway in *Drosophila*. *Genes Dev.* **24**, 2499-2504.
Harris, A. N. and Macdonald, P. M. (2001). Aubergine encodes a *Drosophila* polar granule component required for pole cell formation and related to eIF2C. *Development* **128**, 2823-2832.
Houwing, S., Kamminga, L. M., Berezikov, E., Cronembold, D., Girard, A., van den Elst, H., Filippov, D. V., Blaser, H., Raz, E., Moens, C. B. et al. (2007). A role for Piwi and piRNAs in germ cell maintenance and transposon silencing in zebrafish. *Cell* **129**, 69-82.
Kidwell, M. G. (1983). Evolution of hybrid dysgenesis determinants in *Drosophila melanogaster*. *Proc. Natl. Acad. Sci. USA* **80**, 1655-1659.
King, R. C. (1970). *Ovarian Development in Drosophila melanogaster*. New York: Academic Press.
Klattenhoff, C., Bratu, D. P., McGinnis-Schultz, N., Koppetsch, B. S., Cook, H. A. and Theurkauf, W. E. (2007). *Drosophila* rasiRNA pathway mutations disrupt embryonic axis specification through activation of an ATR/Chk2 DNA damage response. *Dev. Cell* **12**, 45-55.
Klattenhoff, C., Xi, H., Li, C., Lee, S., Xu, J., Khurana, J. S., Zhang, F., Schultz, N., Koppetsch, B. S., Nowosielska, A. et al. (2009). The *Drosophila* HP1 homolog Rhino is required for transposon silencing and piRNA production by dual-strand clusters. *Cell* **138**, 1137-1149.
Lau, N. C., Seto, A. G., Kim, J., Kuramochi-Miyagawa, S., Nakano, T., Bartel, D. P. and Kingston, R. E. (2006). Characterization of the piRNA complex from rat testes. *Science* **313**, 363-367.
Li, C., Vagin, V. V., Lee, S., Xu, J., Ma, S., Xi, H., Seitz, H., Horwich, M. D., Syrzycka, M. and Honda, B. M. (2009). Collapse of germline piRNAs in the absence of Argonaute3 reveals somatic piRNAs in flies. *Cell* **137**, 509-521.
Lim, A. K. and Kai, T. (2007). Unique germ-line organelle, nuage, functions to repress selfish genetic elements in *Drosophila melanogaster*. *Proc. Natl. Acad. Sci. USA* **104**, 6714-6719.
Liu, H., Wang, J. Y., Huang, Y., Li, Z., Gong, W., Lehmann, R. and Xu, R. M. (2010). Structural basis for methylarginine-dependent recognition of Aubergine by Tudor. *Genes Dev.* **24**, 1876-1881.
Malone, C. D. and Hannon, G. J. (2009). Small RNAs as guardians of the genome. *Cell* **136**, 656-668.
Malone, C. D., Brennecke, J., Dus, M., Stark, A., McCombie, W. R., Sachidanandam, R. and Hannon, G. J. (2009). Specialized piRNA pathways act in germline and somatic tissues of the *Drosophila* ovary. *Cell* **137**, 522-535.
Margolis, J. and Spradling, A. (1995). Identification and behavior of epithelial stem cells in the *Drosophila* ovary. *Development* **121**, 3797-3807.
Maurer-Stroh, S., Dickens, N. J., Hughes-Davies, L., Kouzarides, T., Eisenhaber, F. and Ponting, C. P. (2003). The Tudor domain 'Royal Family': Tudor, plant Agenet, Chromo, PWWP and MBT domains. *Trends Biochem. Sci.* **28**, 69-74.
Morrison, S. J. and Spradling, A. C. (2008). Stem cells and niches: mechanisms that promote stem cell maintenance throughout life. *Cell* **132**, 598-611.
Navarro, C., Puthalakath, H., Adams, J. M., Strasser, A. and Lehmann, R. (2004). Egalitarian binds dynein light chain to establish oocyte polarity and maintain oocyte fate. *Nat. Cell Biol.* **6**, 427-435.
Navarro, C., Bullock, S. and Lehmann, R. (2009). Altered dynein-dependent transport in piRNA pathway mutants. *Proc. Natl. Acad. Sci. USA* **106**, 9691-9696.
Nishida, K. M., Okada, T. N., Kawamura, T., Mituyama, T., Kawamura, Y., Inagaki, S., Huang, H., Chen, D., Kodama, T., Siomi, H. et al. (2009). Functional involvement of Tudor and dPRMT5 in the piRNA processing pathway in *Drosophila* germlines. *EMBO J.* **28**, 3820-3831.
Okamura, K., Balla, S., Martin, R., Liu, N. and Lai, E. C. (2008). Two distinct mechanisms generate endogenous siRNAs from bidirectional transcription in *Drosophila melanogaster*. *Nat. Struct. Mol. Biol.* **15**, 998.
Olivieri, D., Sykora, M. M., Sachidanandam, R., Mechtler, K. and Brennecke, J. (2010). An in vivo RNAi assay identifies major genetic and cellular requirements for primary piRNA biogenesis in *Drosophila*. *EMBO J.* **29**, 3301-3317.
Pane, A., Wehr, K. and Schupbach, T. (2007). zucchini and squash encode two putative nucleases required for rasiRNA production in the *Drosophila* germline. *Dev. Cell* **12**, 851-862.
Pelisson, A. (1981). The I-R system of hybrid dysgenesis in *Drosophila melanogaster*: are I factor insertions responsible for the mutator effect of the I-R interaction? *Mol. Gen. Genet.* **183**, 123-129.
Pelisson, A., Sarot, E., Payen-Groschene, G. and Bucheton, A. (2007). A novel repeat-associated small interfering RNA-mediated silencing pathway downregulates complementary sense gypsy transcripts in somatic cells of the *Drosophila* ovary. *J. Virol.* **81**, 1951-1960.
Prud'homme, N., Gans, M., Masson, M., Terzian, C. and Bucheton, A. (1995). Flamenco, a gene controlling the gypsy retrovirus of *Drosophila melanogaster*. *Genetics* **139**, 697-711.
Reuter, M., Chuma, S., Tanaka, T., Franz, T., Stark, A. and Pillai, R. S. (2009). Loss of the Mili-interacting Tudor domain-containing protein-1 activates transposons and alters the Mili-associated small RNA profile. *Nat. Struct. Mol. Biol.* **16**, 639-646.
Roignant, J. Y., Hamel, S., Janody, F. and Treisman, J. E. (2006). The novel SAM domain protein Aveugle is required for Raf activation in the *Drosophila* EGF receptor signaling pathway. *Genes Dev.* **20**, 795-806.
Rorth, P. (1998). Gal4 in the *Drosophila* female germline. *Mech. Dev.* **78**, 113-118.
Roth, S. and Schupbach, T. (1994). The relationship between ovarian and embryonic dorsoventral patterning in *Drosophila*. *Development* **120**, 2245-2257.
Rubin, G. M. and Spradling, A. C. (1982). Genetic transformation of *Drosophila* with transposable element vectors. *Science* **218**, 348-353.
Rubin, G. M., Kidwell, M. G. and Bingham, P. M. (1982). The molecular basis of P-M hybrid dysgenesis: the nature of induced mutations. *Cell* **29**, 987-994.
Saito, K., Inagaki, S., Mituyama, T., Kawamura, Y., Ono, Y., Sakota, E., Kotani, H., Asai, K., Siomi, H. and Siomi, M. C. (2009). A regulatory circuit for piwi by the large Maf gene traffic jam in *Drosophila*. *Nature* **461**, 1296-1299.
Saito, K., Ishizu, H., Komai, M., Kotani, H., Kawamura, Y., Nishida, K. M., Siomi, H. and Siomi, M. C. (2010). Roles for the Yb body components Armitage and Yb in primary piRNA biogenesis in *Drosophila*. *Genes Dev.* **24**, 2493-2498.
Sarot, E., Payen-Groschêne, G., Bucheton, A. and Pélisson, A. (2004). Evidence for a piwi-dependent RNA silencing of the gypsy endogenous retrovirus by the *Drosophila melanogaster* flamenco gene. *Genetics* **166**, 1313-1321.
Shaw, N., Zhao, M., Cheng, C., Xu, H., Saarikettu, J., Li, Y., Da, Y., Yao, Z., Silvennoinen, O., Yang, J. et al. (2007). The multifunctional human p100 protein 'hooks' methylated ligands. *Nat. Struct. Mol. Biol.* **14**, 779-784.
Siomi, M. C., Mannen, T. and Siomi, H. (2010). How does the royal family of Tudor rule the PIWI-interacting RNA pathway? *Genes Dev.* **24**, 636-646.
Song, X., Zhu, C. H., Doan, C. and Xie, T. (2002). Germline stem cells anchored by adherens junctions in the *Drosophila* ovary niches. *Science* **296**, 1855-1857.
Spradling, A. C. (1993). Developmental genetics of oogenesis. In *Development of Drosophila melanogaster* (ed. M. Bate and A. Martinez-Arias), pp. 1-70. Cold Spring Harbor, NY: Cold Spring Harbor Press.
Theurkauf, W. E., Klattenhoff, C., Bratu, D. P., McGinnis-Schultz, N., Koppetsch, B. S. and Cook, H. A. (2006). rasiRNAs, DNA damage, and embryonic axis specification. *Cold Spring Harb. Symp. Quant. Biol.* **71**, 171-180.
Vagin, V. V., Sigova, A., Li, C., Seitz, H., Gvozdev, V. and Zamore, P. D. (2006). A distinct small RNA pathway silences selfish genetic elements in the germline. *Science* **313**, 320-324.
Vagin, V. V., Wohlschlegel, J., Qu, J., Jonsson, Z., Huang, X., Chuma, S., Girard, A., Sachidanandam, R., Hannon, G. J. and Aravin, A. A. (2009). Proteomic analysis of murine Piwi proteins reveals a role for arginine methylation in specifying interaction with Tudor family members. *Genes Dev.* **23**, 1749-1762.
Van Doren, M., Williamson, A. L. and Lehmann, R. (1998). Regulation of zygotic gene expression in *Drosophila* primordial germ cells. *Curr. Biol.* **8**, 243-246.

Wang, J., Saxe, J. P., Tanaka, T., Chuma, S. and Lin, H. (2009). Mili interacts with tudor domain-containing protein 1 in regulating spermatogenesis. *Curr. Biol.* **19**, 640-644.
Wilson, J. E., Connell, J. E. and Macdonald, P. M. (1996). *aubergine* enhances *oskar* translation in the *Drosophila* ovary. *Development* **122**, 1631-1639.
Xie, T. and Spradling, A. C. (1998). *decapentaplegic* is essential for the maintenance and division of germline stem cells in the *Drosophila* ovary. *Cell* **94**, 251-260.
Xu, T. and Rubin, G. M. (1993). Analysis of genetic mosaics in developing and adult *Drosophila* tissues. *Development* **117**, 1223-1237.
Zaccai, M. and Lipshitz, H. D. (1996). Role of Adducin-like (hu-li tai shao) mRNA and protein localization in regulating cytoskeletal structure and function during *Drosophila* Oogenesis and early embryogenesis. *Dev. Genet.* **19**, 249-257.
Zhang, Y. and Kalderon, D. (2001). Hedgehog acts as a somatic stem cell factor in the *Drosophila* ovary. *Nature* **410**, 599-604.

Table S1. *vret* allelic series and molecular lesions

vret allele	Base pair change	Amino acid change	Phenotype over Deficiency	Allelic strength
$vret^{15}$	C799→T	Q267→stop	sterile	strong
$vret^{18}$	C1876→T	Q626→stop	sterile	strong
$vret^{148\text{-}60}$	A1606→C	I536→L	sterile	strong
	C1609→A	Q537→K		
	T1907→A	L636→stop		
$vret^{70}$	G1955→A	W652→stop	spindle	intermediate
$vret^{39}$	G1220→A	G407→E	spindle	intermediate
$vret^{46}$	G797→A	C266→Y	spindle	intermediate/ weak
$vret^{49}$	C1805→T	P602→L	spindle	weak
$vret^{148\text{-}15}$	G1829→A	G610→E	spindle	weak

The location of molecular lesions of each *vret* allele, and the correlation between the severity of the mutation and the phenotypic allelic strength are shown. $vret^{15}$, $vret^{18}$ and $vret^{148\text{-}60}$ females homozygous or transheterozygous with the *vret* deficiency (*Df(3R)Exel6192*) do not produce eggs and exhibit GSC differentiation defects. $vret^{70}$ *and* $vret^{39}$ females transheterozygous with *Df(3R)Exel6192* produce all spindle eggs, and these eggs fail to hatch. $vret^{70}$, $vret^{39}$ and $vret^{46}$ females in trans to *Df(3R)Exel6192* exhibit egg chamber patterning defects. $vret^{46}$, $vret^{49}$ and $vret^{148\text{-}15}$ females transheterozygous with the deficiency produce a percentage of ventralized eggs, as well as fertile eggs. $vret^{49}$ and $vret^{148\text{-}15}$ have no apparent oogenesis defects.

Table S2. *vret* germline clones and quantification of eggshell phenotypes

Genotype	Wild-type phenotype (%)	Ventralized phenotype (%)	Spindle (no DA) (%)	Fused DA (%)
wt	100	0	0	0
$vret^{15}$	1	99	93	6
$vret^{18}$	0	100	84	16
$vret^{148\text{-}60}$	13	87	26	61
$vret^{70}$	45	55	4	51
$vret^{39}$	34	66	14	52
$vret^{46}$	44	56	8	48
$vret^{49}$	45	55	18	37

Germline clones of *vret* alleles (using the ovo^{D} system) produce eggs with different degrees of ventralization, reflecting the strength of the allele (see Table S1). Defining features of the eggshell are the two filamentous structures on the dorsal anterior side, called dorsal appendages (DA). Within the ventralized phenotype, embryos can be spindle (no DA) or have fused DA. *vret* females produce eggs having fused DA or that are completely ventralized (spindle, no DA). For each genotype, 90-120 eggs were analyzed.

Table S3. Expression of *vret* in both germline and somatic tissue rescues fertility

Tissue	Driver tested	Rescue GSC differentiation defects	Rescue somatic defects	Rescue to fertility
germline	*nos-Gal4-VP16*	no	no	no
	otu-Gal4	no	no	no
soma	*c587-Gal4*	yes	yes	no
	traffic jam-Gal4	yes	yes	no
	bab1-Gal4	no	no	no
whole fly	*actin5c-Gal4*	yes	yes	yes

Ovarian phenotypes exhibited in $vret^{148\text{-}60}$ mutants were rescued to different extent by expressing a *UASp-vret-myc* transgene in germline, ovarian somatic tissue or the whole fly. Sterility, measured by production of viable progeny, was only rescued when *vret* was expressed in both germline and soma.

Table S4. Transposable elements tested in microarray analysis in *vret*, *piwi* and *aub* mutant ovaries.

Order #	Name	Affymetrix Probe Set ID	RQ vret/vret vs vret/TM6	RQ piwi/piwi vs piwi/CyO	RQ aub/aub vs aub/CyO	Chromosome strand	Chromosome number	Chromosome Start Index	Chromosome End Index	Representative Public ID
1	176	1626392_s_at	20.53	2.38	0.42	+	chr2RHet	853622	861122	Transposon.2
2	1731	1625050_s_at	103.75	6.01	1.24	+	chr3LHet	854127	858777	Transposon.3
3	Juan	1626966_s_at	109.95	5.77	1.43	+	chr2LHet	123504	127732	Transposon.82
4	invader4	1625791_s_at	8.87	2.32	1.08	+	chrUextra	1002853	1004084	Transposon.68
5	P-element	1628989_at	12.58	1.93	1.05		NA	NA	NA	Transposon.27
6	Stalker3	1627940_at	1.54	1.12	1.00	+	chrYHet	136646	137018	Transposon.98
7	Tirant	1640955_s_at	7.72	1.12	1.01	+	chr2L	21041188	21049393	Transposon.34
8	Ivk	1629641_s_at	92.28	1.42	1.43	+	chr2LHet	237707	243077	Transposon.65
9	G6	1626205_s_at	36.05	1.54	1.54	+	chrUextra	14612123	14984929	Transposon.90
10	Bari1	1637622_s_at	15.11	6.42	1.15	+	chr2RHet	1422686	1424414	Transposon.8
11	TARTelement[1]	1638428_at	13.72	4.89	1.25	+	chrU	4022445	7585147	Transposon.33
12	TARTelement[2]	1629242_x_at	12.91	6.63	1.24	+	chrU	4022445	7585147	Transposon.33
13	Quasimodo	1635258_s_at	25.26	14.55	1.81	+	chr3LHet	956252	963255	Transposon.46
14	gypsy2	1635829_s_at	2.80	2.17	1.23	+	chr2RHet	2362644	2370556	Transposon.53
15	Stalker2	1636015_s_at	343.43	48.32	3.72	+	chr3L	14818280	14825950	Transposon.97
16	mdg1	1625195_s_at	20.94	48.77	0.90	+	chr2R	20615461	20622912	Transposon.24
17	ZAM[1]	1634666_at	211.72	247.15	1.05	+	chrU	1399231	1407666	Transposon.39
18	ZAM[2]	1640448_x_at	202.14	201.53	0.99	+	chrU	1399231	1407666	Transposon.39
19	GATE	1623960_s_at	42.64	37.39	1.00	+	chrU	3879370	8878422	Transposon.40
20	gypsy5	1626434_s_at	70.42	104.72	0.74	-	chrX	11088516	11095880	Transposon.75
21	Tabor	1631349_s_at	736.43	253.59	1.24	+	chr2RHet	905661	913014	Transposon.49
22	transib1	1630262_s_at	33.23	21.35	1.05	+	chr3LHet	220943	222786	Transposon.72
23	Dm88	1634187_x_at	80.32	107.10	2.43	+	chrXHet	128219	132719	Transposon.81
24	gtwin	1637055_s_at	2.25	9.35	0.96	-	chrX	1522061	1529472	Transposon.52
25	gypsy6	1635017_at	12.12	140.98	0.81	+	chrU	2236387	2243897	Transposon.76
26	diver2	1641421_s_at	1.25	1.55	0.95	+	chr2RHet	3145061	3149747	Transposon.78
27	invader3	1627936_s_at	5.84	16.89	1.70	+	chr3R	3533255	3539357	Transposon.59
28	looper1	1623159_at	1.38	1.60	0.97	+	chr2R	2352600	2354454	Transposon.91
29	412	1640167_s_at	11.99	3.35	4.94	+	chrX	927439	935015	Transposon.6
30	accord	1634633_s_at	55.32	8.98	10.71	-	chrU	2407801	2415206	Transposon.54
31	McClintock	1635696_s_at	76.96	5.12	11.22	+	chr2LHet	330880	337332	Transposon.94
32	blastopia	1639729_s_at	111.05	16.00	35.75	+	chr2L	20407864	20412893	Transposon.35
33	blood	1635886_s_at	83.93	12.75	41.15	+	chr3RHet	845661	853073	Transposon.38
34	rover	1624377_s_at	82.16	9.74	47.67	+	chr2RHet	2992919	3001325	Transposon.84
35	Burdock	1633959_s_at	334.11	73.07	40.93	+	chr2RHet	30696	37111	Transposon.10
36	Transpac	1640242_s_at	189.24	154.81	54.54	+	chr2RHet	680778	692162	Transposon.42
37	HMS-Beagle	1633998_s_at	337.25	205.28	334.93	+	chr3LHet	2202218	2209278	Transposon.47
38	Cr1a	1640606_x_at	2.19	1.82	1.47	+	chr2RHet	1337960	3131796	Transposon.61
39	Doc2-element	1632295_s_at	2.10	1.64	1.31	+	chr2RHet	2408043	3084366	Transposon.63
40	micropia	1641450_s_at	2.41	1.40	1.52	+	chr3RHet	1080748	1088869	Transposon.26
41	Rt1b	1623349_x_at	4.61	1.39	1.78	+	chr3LHet	1877419	1881467	Transposon.45
42	Doc3-element	1630948_s_at	5.54	1.34	2.61	+	chr3RHet	717935	1950212	Transposon.64
43	Arc2	1632639_at	2.08	0.90	1.36	+	chr2R	10249448	10250330	CG13941-RA
44	copia	1632683_s_at	3.97	7.61	3.72	+	chr3LHet	666602	671748	Transposon.11
45	HeT-A[1]	1630585_s_at	5.36	41.77	9.35	-	chr4	1286271	1311469	Transposon.20
46	R2-element	1630934_at	1.79	4.78	3.97	+	chrXHet	198909	202495	Transposon.30
47	HeT-A[2]	1624224_at	1.52	10.27	3.65	-	chr4	1286271	1311469	Transposon.20
48	springer	1624543_s_at	2.06	71.73	4.29	+	chr2RHet	2930065	2935915	Transposon.32
49	opus	1638469_s_at	2.48	18.06	2.45	+	chr2RHet	2204719	2212330	Transposon.36
50	Arc1	1639694_s_at	1.56	0.87	1.54	-	chr2R	10248808	10249506	CG10102-RA
51	pogo	1639054_s_at	22.30	0.18	3.44	+	chr2L	7959094	7960043	Transposon.28
52	gypsy	1624819_s_at	13.40	6.44	0.01	+	chr3L	24456688	24464149	Transposon.17
53	R1-element	1637786_s_at	1.64	1.03	0.43	+	chrUextra	21133846	23681524	Transposon.29
54	frogger	1625649_s_at	0.74	0.76	0.99	+	chr3RHet	77163	88643	Transposon.83
55	CG31617	1629740_at	0.14	0.32	0.99	+	chrUextra	10958515	11389945	CG31617-RA

Average relative quantities (RQ) of transposon mRNAs (55 array probe set IDs, 52 unique transposons) expressed as ratios of levels in homozygous compared with heterozygous ovaries (two biological replicates were profiled per genotype). The order # corresponds to the order (left to right) of the same transcripts in unsupervised hierarchical clustering heat maps shown in Fig. 3J.